HHS Public Access

Author manuscript

Int J Biochem Cell Biol. Author manuscript; available in PMC 2017 September 01.

Published in final edited form as:

Int J Biochem Cell Biol. 2016 September ; 78: 149–155. doi:10.1016/j.biocel.2016.06.018.

Inositol hexakisphosphate kinase-1 interacts with perilipin1 to modulate lipolysis

Sarbani Ghoshal[1], **Richa Tyagi**[2], **Qingzhang Zhu**[1], and **Anutosh Chakraborty**[1,*]

[1]Department of Metabolism and Aging, The Scripps Research Institute, Jupiter, FL 33458, USA

[2]The Solomon H. Snyder Department of Neuroscience, Johns Hopkins University School of Medicine, Baltimore, MD 21205, USA

Abstract

Lipolysis leads to the breakdown of stored triglycerides (TAG) to release free fatty acids (FFA) and glycerol which is utilized by energy expenditure pathways to generate energy. Therefore, a decrease in lipolysis augments fat accumulation in adipocytes which promotes weight gain. Conversely, if lipolysis is not complemented by energy expenditure, it leads to FFA induced insulin resistance and type-2 diabetes. Thus, lipolysis is under stringent physiological regulation although, the precise mechanism of the regulation is not known. Deletion of inositol hexakisphosphate kinase-1 (IP6K1), the major inositol pyrophosphate biosynthetic enzyme, protects mice from high fat diet (HFD) induced obesity and insulin resistance. IP6K1-KO mice are lean due to enhanced energy expenditure. Therefore, IP6K1 is a target in obesity and type-2 diabetes. However, the mechanism/s by which IP6K1 regulates adipose tissue lipid metabolism is yet to be understood. Here, we demonstrate that IP6K1-KO mice display enhanced basal lipolysis. IP6K1 modulates lipolysis *via* its interaction with the lipolytic regulator protein perilipin1 (PLIN1). Furthermore, phosphorylation of IP6K1 at a PKC/PKA motif modulates its interaction with PLIN1 and lipolysis. Thus, IP6K1 is a novel regulator of PLIN1 mediated lipolysis.

Introduction

A coordinated stimulation of lipolysis and energy expenditure is beneficial in reducing adipose mass without causing insulin resistance (Ahmadian M, 2009; Boden, 2008; Langin, 2006). Insulin inhibits lipolysis whereas catecholamine like adrenaline stimulate the process by the β-AR/PKA (β-adrenergic receptor-protein kinase A) mediated regulation of lipolytic enzymes and regulators (Langin, 2006). Various enzymes are involved in hydrolyzing TAG to FFA *via* intermediate production of DAG (diglycerides) and MAG (monoglycerides). ATGL (adipose TAG lipase) converts TAG to DAG; HSL (hormone sensitive lipase) generates TAG to DAG and DAG to MAG; and MGL (monoacyl glycerol lipase) works on the last step to release FFA and glycerol (Young SG, 2013). In addition, proteins such as

[*]**Contact information:** achakrab@scripps.edu. Phone: 561-228-2426, Fax: 561-228-3059.

perilipin (PLIN) and CGI-58 regulate lipolysis by modulating activities of the lipases (Young SG, 2013). CGI-58 stimulates lipolysis by enhancing ATGL activity (Young SG, 2013). PLINs are a family of proteins of which PLIN1 is the most studied (Brasaemle, 2007). PLIN1 binds and inhibits CGI-58's stimulatory action on ATGL and thus, inhibits basal lipolysis. β-AR stimulation/PKA activation phosphorylates PLIN1 to disrupt its association with CGI-58. Phosphorylated PLIN1 binds and stimulates HSL mediated lipolysis. PLIN1-KO mice are resistant to obesity and they display high basal but impaired β-AR induced lipolysis (Tansey JT, 2001). These mice also exhibit enhanced β-oxidation and UCP1 expression (Saha PK, 2004). Moreover, PLIN1 deletion reverses obesity in ob/ob mice (Martinez-Botas J, 2000). PLIN2-KO mice are also protected against diet induced obesity, fatty liver and inflammation presumably *via* increased browning and decreased food intake (McManaman JL, 2013). On the other hand, PLIN1 loss of function mutation causes increased basal lipolysis, lipodystrophy and insulin resistance in humans (Kozusko K, 2013) which is explainable as the balance between lipolysis and energy expenditure is disturbed which is important to maintain insulin sensitivity. Thus, targeting PLIN1 and energy expenditure is beneficial in obesity and diabetes. However, *in vivo* regulation of PLIN1 is not known. It is also not known whether a common regulator exists that coordinates PLIN1/ lipolysis and energy expenditure *in vivo*.

IP6K1 generates the signaling molecule, inositol pyrophosphate, commonly known as 5-IP7 (Chakraborty A, 2011; Saiardi A, 1999; Wilson MS, 2013). Functions of three mammalian IP6K isoforms (IP6K1-3; of which IP6K1 is the major isoform (Chakraborty A, 2011; Wilson MS, 2013) are currently being explored (Chakraborty A, 2011). Although, IP6Ks display conserved active sites, they possess unique regulatory regions which mediate specific protein-protein interactions (Barker CJ, 2009; Chakraborty A, 2011). Accordingly, IP6Ks exhibit different functions (Chakraborty A, 2011; Morrison BH, 2009). IP6K1 generated 5-IP7 facilitates insulin secretion (Illies C, 2007). IP6K2 regulates apoptosis and cancer metastasis (Chakraborty A, 2011; Koldobskiy MA, 2010; Morrison BH, 2009; Rao F, 2015) whereas IP6K3 modulates synapse formation in cerebellar Purkinje cells (Fu C, 2015).

Mice deleted of IP6K1 are insulin hypersensitive on chow-diet (Bhandari R, 2008). In addition, IP6K1-KO mice are protected against high fat diet (HFD) induced obesity, insulin resistance, hyperinsulinemia, hypertriglyceridemia and fatty liver (Chakraborty A, 2010). Aged and HFD-fed IP6K1-KO mice maintain insulin sensitivity due to the loss of 5-IP7's inhibitory action on the insulin sensitizing protein kinase Akt (Chakraborty A, 2010). 5-IP7 inhibits Akt *in vivo* and *in vitro* (Chakraborty A, 2010; Gokhale NA, 2013; Prasad A, 2011; Wu M, 2013; Xu Y, 2013; Zhang Z, 2014a; Zhang Z, 2014b). Moreover, IP6K1-KO mice are lean due to enhanced energy expenditure as energy intake is unaltered in these mice (Chakraborty A, 2010). Therefore, IP6K1 is a target in obesity/T2D (Boucher J, 2014; Chakraborty A, 2011; Mackenzie RW, 2014; Shears, 2016). However, the precise mechanism/s by which IP6K1 regulates lipid metabolism in not known. Here, we demonstrate that IP6K1 is a novel regulator of lipolysis. Furthermore, IP6K1 modulates lipolysis by phosphorylation mediated interaction with PLIN1.

Materials and Methods

Materials

Antibodies: pPKA and pPKC substrate specific antibodies; PLIN1 and pHSL (S660): from Cell Signaling Technology. CGI-58, HSL, GST and β-Actin: from Santa Cruz Biotechnology. Myc: from Roche. IP6K1: from Genetex. **Plasmid construct:** pT7T3D-PacI-PLIN1 construct was purchased from GE Healthcare/Open Biosystems. **Reagents and Kits:** Glycerol, FFA and TAG assay kits: from Cayman Chemicals; insulin Elisa kit from Crystal Chem; BCA protein assay kit: Pierce Biotechnology; Jetprime transfection reagent from Polypus; RetroX concentrator: from Clontech; Cyclic AMP from Cell Signaling; protein A/G beads from EMD Millipore. **Pharmacologic modulators:** Forskolin/FSK (Cell Signaling), isoproterenol (Sigma), CL316243 (Sigma); Rottlerin, LY333531 and GF109203X (Tocris). Protease plus phosphatase inhibitor tablets; Thermo Scientific, Waltham, MA. Unless otherwise stated, all the chemicals are purchased from Sigma Aldrich.

Animals

Six to eight weeks old male WT and IP6K1-KO mice were housed under barrier conditions with standard chow diet (CD) (Harlan Laboratories # 2018SX) and water provided *ad libitum*. Animals were maintained at 12hr light–dark cycle at ambient temperature of 23°C. All protocols were approved by the Scripps Florida, Institutional Animal Care and Use Committee.

Tissue Collection

Mice were euthanized by carbon dioxide asphyxiation (ARC Facility, Scripps Florida). For end point studies, blood was collected by cardiac puncture for plasma preparation. Fat pads were snap-frozen in liquid nitrogen and stored at −80°C for measuring protein expression by immunoblotting or for immunoprecipitation studies.

Lipolysis Studies

Basal and Isoproterenol induced: Isoproterenol treatment was done following a standard protocol (Qiao L, 2011). Briefly, isoproterenol was injected intraperitoneally to overnight fasted mice at 5 mg/kg body weight. Blood samples were collected 20mins before (basal) and after (stimulated) injection in vacutainer plasma preparation tubes. Blood was spun at 1500g for 10 min at 4°C and plasma was aliquoted and stored at −80°C. Plasma was analyzed for Glycerol and FFA using kits from Cayman Chemicals for each parameter. **Basal and CL316243 induced:** CL316243 was injected in *ad libitium* mice intraperitoneally (0.5 mg/kg body weight). Blood was collected immediately before and 30 minutes after injection (Roth Flach RJ, 2013). **In adipose tissue explants:** To measure lipolysis in explants *in vitro*, standard procedure was followed (Taschler U, 2011) with slight modifications suggested by the Zechner laboratory. Briefly, equal weights of EWAT, IWAT and RWAT were taken into a 96-well plate with 200 μl media. The plate was incubated at 37°C for 2h with gentle shaking (basal lipolysis). Thereafter, samples were transferred to a fresh plate containing media with 10 μM isoproterenol and incubated for 30 min. Finally, fat pads were transferred to another fresh plate having media and isoproterenol and was

incubated for 1h (stimulated lipolysis). **In 3T3L1 adipocytes:** Fully differentiated 3T3L1 adipocytes were treated with DMEM containing 0.5% Fatty Acid Free BSA (Sigma) for four hours, and this media was collected for basal lipolysis measurement. Thereafter, cells were treated with 10μM isoproterenol for 1 hour and the media was collected for measurement of stimulated lipolysis (Gauthier MS, 2008).

Measurement of plasma insulin following CL316243 treatment

CL316243 treated plasma was obtained as described in the lipolysis section. Plasma was used to measure insulin levels as per manufacturer's instructions.

Plasma triglyceride analysis

Plasma was isolated from WT and IP6K1-KO mice and triglyceride was measured as per manufacturer's instructions.

Mass spectrometry to identify IP6K1 interacting proteins in 3T3L1 adipocytes

3T3L1 preadipocytes overexpressing Myc–IP6K1 and control vector were differentiated for 8 days. Afterwards, cells were lysed using lysis buffer (containing protease and phosphatase inhibitors). One mg of the lysate was pre-cleared with IgG and Protein A/G beads. Thereafter, the supernatant was incubated with IgG or Myc-antibody and Protein A/G beads overnight. Samples were spun down, supernatant was discarded and beads were washed 3× with wash buffer. Immunoprecipiated IgG control and Myc-IP6K1 interactors were separated in a SDS-PAGE gel. Bands that were specifically co-immunopripitated with Myc-IP6K1 were cut and submitted for mass spectrometry based identification. Corresponding bands from IgG control were also sequenced. Proteins identified only in Myc-IP6K1 samples were confirmed as IP6K1 interactors.

Mass spectrometry to identify IP6K1 interactome in the IWAT

For immunoprecipitation of endogenous IP6K1 from IWAT, total protein was extracted from the tissue using lysis buffer. Immunoprecipitation was performed following the same procedure as described above. IgG and IP6K1 antibodies were used for this experiment. The washed beads were processed at the mass spectrometry facility to identify all the binding proteins for IgG and IP6K1. Proteins detected in both the samples were considered as non-specific binders. Protein only/majorly bound to IP6K1 are considered as IP6K1 interactors.

For mass spectrometry, samples were subjected to SDS-PAGE at 70V for 25 min. The gel was Coomassie stained for 1 hour at room temperature with shaking, followed by destaining in water overnight. The gel bands were cut, in-gel treated with 10 mM DTT followed by 50 mM iodoacetamide, and subjected to trypsin digestion overnight. Prior to mass spectrometry analysis, the peptide pools were acidified, desalted through Zip-Tip C18 tip columns and dried down. Each sample was reconstructed in 100 μl of 0.1% formic acid and 13μl were loaded into the system.

Each sample was analyzed by liquid-chromatography-tandem MS (LC-MS/MS) using an EASY-nLC 1000 system coupled to a Q Exactive mass spectrometer (Thermo Fisher Scientific). Peptides were concentrated and desalted on an RP pre-column (0.075 × 20 mm

Acclaim PepMap 100 nano Viper, Thermo Fisher Scientific) and on-line eluted on an analytical RP column (0.075 × 150 mm Acclaim PepMap RLSC nano Viper, Thermo Fisher Scientific), operating at 300 nl/min using the following gradient: 5% B for 3 min, 5–40% B in 60 min, 40–80% B in 2 min, and 80% B for 9 min, 80–5% B for 30 sec, and 5% B for 5 min [solvent A: 0.1% formic acid (v/v); solvent B: 0.1% formic acid (v/v), 80% CH3CN (v/v) (Fisher Scientific)]. The Q Exactive was operated in a data-dependent MS/MS mode using the 10 most intense precursors detected in a survey scan from 380 to 1,600 m/z performed at 70K resolution. Tandem MS was performed by HCD fragmentation with normalized collision energy (NCE) of 27.0%. Protein identification was carried out using Mascot and Sequest algorithms. MS/MS raw files were searched against a Mouse database which also includes human keratins and porcine trypsin.

Mass spectrometric identification of IP6K1 phosphorylation at serines 118 and 121

GST-IP6K1 was pulled down from HEK293 cells and were submitted to Taplin Mass Spectrometry Facility at Harvard University to detect its posttranslational modifications.

PLIN1 sub-cloning

Mouse PLIN1 cDNA was purchased from Open Biosystems. PLIN1 was PCR amplified and cloned into pCMV-Myc vector at the SalI-NotI restriction sites.

GST-Pull down assays

HEK cells were co-transfected with Myc-PLIN1 along with GST, GST-IP6K1 WT, DM (SS118A/S121AA) or S85A-IP6K1 at 80% confluence. 48 hours post transfection, cells were washed with PBS, and cells were scraped on ice with lysis buffer (200mM NaCl and 20mM Tris-HCl, 1% Triton × with protease+phosphatase inhibitor tablet). The cell supernatant concentration was determined using BCA reagents. 750ug of the lysate was incubated with glutathione beads (Thermo Scientific) overnight, washed thrice with lysis buffer (without inhibitor) and eluted with LDS sample loading buffer containing 5% β-mercaptoethenol. Samples were heated, spun down and run on a 4–12% Bis-Tris gel and blotted with Myc and GST.

Cell Culture

3T3-L1 cells (passage<6), HEK 293 cells were cultured in DMEM high glucose media (GIBCO) supplemented with 10% heat-inactivated serum and 1% Pen-Strep. 3T3-L1 cells were differentiated following standard protocol (Zebisch K, 2012). For over-expression studies, 3T3L1 preadipocytes were transduced following standard protocol (Chakraborty A, 2010). Transduced cells were differentiated following standard protocol.

PKC/PKA modulator treatments in cell culture

Forskolin (FSK; 50 μM) was treated for indicated time periods. PMA (500 nM) was treated for 3h. GF109203X (500 nM), LY333531 (500 nM) and rottlerin (2 μM) was treated for 30 min.

Retroviral overexpression of Myc-IP6K1-WT and Myc-IP6K1-DM in 3T3L1 adipocytes

Cloning of Myc-IP6K1 WT and DM versions in the retrovial vector pMXIRES were performed following standard procedures (Chakraborty A, 2010). Platinum E (Plat-E) cells were transfected with control vector, IP6K1-WT or DM plasmids. After two days, supernatant media was collected and mixed with retrovirus concentration reagent from Clontech in the ratio 3:1. The mixture was incubated overnight at 4°C and thereafter centrifuged at 1500g for 45mins at 4°C. After centrifugation, all supernatant was discarded carefully, pellet was resuspended in PBS and stored in small aliquots at −80°C. Equal level of protein expression of IP6K1-WT and IP6K1-DM were standardized by transducing various volumes of purified virus. Finally, 3T3-L1 cells were transduced and thereafter differentiated.

SDS-PAGE and Immunoblotting

For immunoblotting, protein was isolated by standard protein lysis buffer containing protease-phosphatase inhibitor (Thermo-Scientific) and quantified using a BCA protein assay kit (Pierce). Immunoblotting was performed following standard procedures (Chakraborty et al 2008).

Statistical Analysis

Mouse number is indicated in each experiment. Statistical analysis was done with GraphPad Prism software version 6. For multiple comparisons, two-way Anova with Tukey's multiple comparison was used. For two independent data sets, two tailed Student's *t-test* was used. Data are presented as mean ± SEM (****P ≤ 0.0001, ***P ≤ 0.001, **P ≤ 0.01 and *P≤0.05).

Results

IP6K1-KO mice display altered lipolysis

A complete hydrolysis of triglycerides releases the glycerol backbone which is a standard measurement of lipolysis (Lucas S, 2003; Tansey JT, 2001). Plasma glycerol level is higher in the overnight fasted knockouts compared to their WT littermates in absence of the β-AR agonist isoproterenol (Figure 1A; left panel). Isoproterenol induced maximum lipolytic efficiency is slightly hampered in IP6K1-KO mice (Figure 1A; right panel). As a result, the ratio of isoproterenol induced *vs* basal lipolysis is significantly less in the knockouts (Figure 1B). Increased basal lipolysis is also confirmed by higher PKA mediated stimulatory phosphorylation of HSL (serine 660) in IP6K1-KO mice under basal conditions which is not further stimulated following isoproterenol treatment (Figure 1C). However, raw values of FFA is similar in WT and IP6K1-KO mice (Figure S1A). Chow-fed knockouts exhibit 2–3 fold less fat mass than WT (Chakraborty A, 2010). Thus, although the raw values of FFA are unaltered, it is at least doubled in the knockouts, if normalized against fat mass. As observed before (Chakraborty A, 2010), plasma triglyceride level is less in the knockouts (Figure S1B). To assess lipolysis in equal fat masses of WT and IP6K1-KO mice, we measured basal and isoproterenol induced glycerol release in explants isolated from epididymal, inguinal and retroperitoneal adipose tissue depots (EWAT, IWAT and RWAT). Basal glycerol release

is higher whereas isoproterenol induced lipolysis is not significantly altered in the knockout adipose explants (Figure 1D). Therefore, the lipolytic ratio is reduced in the knockout explants similar to what is observed *in vivo* (Figure 1E).

Isoproterenol stimulates β-AR in general whereas the CL316243 compound specifically induces β3-AR in the adipose tissue to stimulate lipolysis (Roth Flach RJ, 2013). Plasma glycerol is slightly higher whereas CL316243 induced glycerol release in partly hampered in ad libitum knockouts (Figures 1F). Thus, the ratio of CL316243 induced *vs* basal lipolysis is lower in the knockouts (Figure 1G). CL316243 enhances insulin secretion (Grujic D, 1997). Conversely, IP6K1 deletion reduces serum insulin level (Bhandari R, 2008; Chakraborty A, 2010). Therefore, we monitored whether CL316243 mediated increase in plasma insulin level is affected in the knockouts. Under basal condition, plasma insulin level is slightly lower in IP6K1-KO mice (Figure 1H; left panel). CL316243 enhances insulin level in both the genotypes (Figure 1H; right panel). However, the enhancement is marginally reduced in the knockouts (Figure 1I).

IP6K1 deletion does not seem to alter global β-AR/PKA signaling as the cAMP level is unaltered in the knockouts (Figure S1C). Expression levels of the lipolytic proteins such as PLIN1, CGI-58 and ATGL are also similar in WT and IP6K1-KO EWAT (Figure S1D). Therefore, we presume that IP6K1 regulates lipolysis *via* a distinct mechanism.

A PKA/PKC phosphorylation motif in IP6K1 regulates its interaction with PLIN1 and lipolysis

To determine the precise mechanism by which IP6K1 regulates lipolysis, we employed a mass spectrometry approach to identify IP6K1 interacting proteins in the adipocytes. In one approach, immunoprecipitation of retrovirally overexpressed Myc-IP6K1 from mature 3T3L1 adipocytes and mass spectrometry were performed to identify its major interactors. In a second approach, all the binding proteins of endogenous IP6K1 in the IWAT were identified by LC-MS/MS. Both experiments reveal that PLIN1 is a major interactor of IP6K1 (Figures 2A, S2A–S2D). We also identified PLIN4 in the IWAT (Figure 2A; bottom panel). Other IP6K1 interacting proteins in the IWAT were also identified which are not directly relevant to this study and thus, will be characterized separately (data not shown). We confirmed IP6K1-PLIN1 interaction in 3T3L1 adipocytes by immunoblotting (Figure 2B).

Next, we determined the molecular mechanism by which IP6K1 interacts with PLIN1. IP6K1 possesses a lipase like motif (Figure 2C; GDSDG; residues 83–87) (Wong H, 2002). Yet, IP6K1 neither displays lipid hydrolase activity nor influences activity of other lipases *in vitro* such as HSL (data not shown). Moreover, mutation of the serine 85 residue in the putative lipase motif does not influence IP6K1's binding to PLIN1 (Figure 2D). IP6K1 also contains a high stringent PKC/PKA phosphorylation motif (serines 118 and 121) (Figure 2C). LC-MS/MS analyses of GST-IP6K1 overexpressed in HEK293 cells reveals that both S118 and S121 residues are phosphorylated in cells. For immunodetection of these phosphorylation sites, we employed phospho-substrate specific antibodies. We used both pPKA and pPKC substrate specific antibodies. Both the antibodies detect IP6K1 phosphorylation in HEK293 cells although the pPKC-substrate antibody detects the motif slightly better. Therefore, we used the pPKC-substrate antibody for the experiments. The

antibody specifically detects phosphorylation of IP6K1 as the other two IP6K isoforms do not cross-react (Figure S2E). Pharmacologic activation of PKC by phorbol ester (PMA) enhances IP6K1 phosphorylation (Figure 2E). Conversely, the pan PKC inhibitor GF109203X or the PKCβ specific inhibitor LY333531 reduces IP6K1 phosphorylation whereas the PKCδ inhibitor rottlerin is ineffective (Figure 2F). In addition to PKC, activation of PKA by forskolin (FSK) also enhances GST-IP6K1 phosphorylation (Figure 2G). Phosphorylation of endogenous IP6K1 in HEK293 cells is enhanced to a greater extent by PKC compared to PKA activation (Figure 2H). Thus, IP6K1 is primarily phosphorylated by PKC in HEK293 cells. To monitor impacts of IP6K1 phosphorylation on PLIN1 binding, we mutated the serines in the phosphorylation motif of the kinase (IP6K1-S118A/S121A; double mutant; IP6K1-DM). The antibody fails to cross-react with IP6K1-DM which confirms that it detects phosphorylation at this motif (Figure 2I). Moreover, IP6K1 phosphorylation is essential for its binding to PLIN1 as IP6K1-DM no longer binds PLIN1 (Figure 2J).

Next, we monitored impacts of IP6K1 phosphorylation on lipolysis. In 3T3L1 adipocytes, endogenous IP6K1 is phosphorylated which is further enhanced by PKC or PKA activation (Figure 2K). Moreover, retroviral overexpression of WT and IP6K1-DM (Figure S2F) reveal that IP6K1 phosphorylation is higher in the mature adipocytes compared to preadipocytes (Figure 2L; WT-IP6K1). As expected, IP6K1-DM mutant is not phosphorylated under any conditions (Figure 2L; IP6K1-DM). Finally, we monitored impacts of PKC/PKA phosphorylation deficient IP6K1 mutant on lipolysis. Contrary to IP6K1 deletion (Figure 1) IP6K1-WT overexpression enhances induced/basal lipolysis in 3T3L1 adipocytes (Figure 2M; red bar) due to decreased basal lipolysis (data not shown). Conversely, the PLIN1-binding deficient IP6K1-DM fails to alter lipolysis (Figure 2N; green bar). Thus, IP6K1 binds PLIN1 *via* a phosphorylation motif which modulate lipolysis.

Discussion

We demonstrate that IP6K1 is a novel regulator of lipolysis. Thus, basal lipolysis is enhanced in IP6K1-KO mice which leads to diminished induced/basal lipolysis in these mice. IP6K1 modulates lipolysis *via* its interaction with PLINs. Furthermore, PKA/PKC phosphorylation of IP6K1 facilitates its binding to PLIN1 which modulates lipolysis. PKA is a major kinase that regulates PLIN1 mediated lipolysis (Ahmadian M, 2009). PKC's role in PLIN1 regulated lipolysis is also currently being appreciated (Thrush AB, 2012).

Therefore, regulation of PLIN1 mediated lipolysis by IP6K1 and its modulation by PKA/PKC phosphorylation bear considerable significance in understanding the basic mechanism of lipolysis. Both PKA and PKC phosphorylate IP6K1 at the same motif. It is possible that anyone/both of them phosphorylate the residues depending on cell type and conditions. For example, PKC seems to phosphorylate IP6K1 more efficiently in HEK293 cells whereas in 3T3L1 adipocytes the extent of phosphorylation by PKC and PKA are somewhat similar. It is to be determined which kinase phosphorylates which residue/s during lipolysis. Our preliminary data indicates that IP6K1 co-localizes with PLIN1 in the endoplasmic reticulum (ER) but not in the lipid droplets of adipose tissue. This is conceivable as IP6K1-PLIN1 binds in lipid-droplet deficient HEK293 cells. Furthermore,

PLIN1 accumulation in the ER is enhanced in IP6K1-KO adipose tissue (Chakraborty lab unpublished observation). PLIN1 is known to translocate from the ER to the lipid droplet during the maturation of the droplets (Skinner JR, 2013). Therefore, it is conceivable that IP6K1-PLIN1 interaction enhances PLIN1 maturation and its translocation to the lipid droplet which is modulated by IP6K1 phosphorylation by PKA/PKC. Current research is ongoing to decipher the molecular mechanism of these interactions and its physiological and pathological significance in obesity and diabetes. In addition to its impacts on lipolysis, PKA/PKC phosphorylation of IP6K1 may also regulate other pathways that are modulated by IP6K1 such as Akt activity and insulin signaling, insulin secretion and glycolysis (Chakraborty A, 2010; Illies C, 2007; Szijgyarto Z, 2011). Thus, our current study reveals that IP6K1-PLIN1 interaction regulates lipid metabolism *via* a novel mechanism in the adipose tissue.

Insulin inhibits lipolysis. Therefore, lower insulin level may also contribute to enhanced lipolysis in the knockouts. Both chow- and HFD-fed knockouts exhibit substantially less fat mass than WT (Chakraborty et al. Cell, 2010). Therefore, glycerol/FFA is derived from less fat mass which further indicates increased lipolysis in the knockouts. Yet, increased lipolysis does not cause insulin resistance in IP6K1-KO mice as the knockouts are insulin hypersensitive under both chow- and HFD-fed conditions. Accordingly, they display efficient glucose uptake following glucose and insulin injections (GTT/ITT) and in hyperinsulinemic euglycemic clamps studies (Bhandari R, 2008; Chakraborty A, 2010). Moreover, IP6K1-KO mice are resistant to HFD-induced weight gain, hypertriglyceridemia and fatty liver (Chakraborty A, 2010). HFD-knockouts also display altered lipolytic efficiency (Chakraborty lab unpublished observation) and increased energy expenditure (Chakraborty A, 2010). Thus, FFA released by lipolysis is efficiently utilized by the knockouts by energy expenditure which reduces fat accumulation without causing insulin resistance. In summary, IP6K1 inhibits insulin mediated glucose uptake (Chakraborty A, 2010) whereas it promotes lipogenic actions of the hormone which causes age or HFD induced lipid accumulation. It is intriguing that IP6K1 regulates insulin mediated glucose homeostasis and lipolysis *via* distinct mechanisms. Thus, IP6K1's impact on these processes can be differentially targeted in metabolic diseases.

Supplementary Material

Refer to Web version on PubMed Central for supplementary material.

Acknowledgments

We sincerely thank Prof. Solomon Snyder for sharing IP6K1-KO mice and various reagents and constructs for the research. We also thank Adele Snowman, Asif Mustafa and Krishna Juluri from Snyder lab for experimental assistance. We thank Prof. Rudolf Zechner's laboratory for sharing their protocol to measure lipolysis in adipose tissue explants and Dr. James G. Granneman for providing critical comments and valuable suggestions. We thank Luise Angelini for experimental assistance. We also thank Pablo Martinez and Catherina Scharager-Tapia at the TSRI proteomic core facility and the TSRI Metabolism and Aging department for sharing reagents and instruments. The work is supported by TSRI startup fund and R01DK103746-01A1.

References

Ahmadian M, D R, Sul HS. The skinny on fat: lipolysis and fatty acid utilization in adipocytes. Trends Endocrinol Metab. 2009; 20:424–428. [PubMed: 19796963]

Barker CJ, I C, Gaboardi GC, Berggren PO. Inositol pyrophosphates: structure, enzymology and function. Cell Mol Life Sci. 2009; 66:3851–3871. [PubMed: 19714294]

Bhandari R, J K, Resnick AC, Snyder SH. Gene deletion of inositol hexakisphosphate kinase 1 reveals inositol pyrophosphate regulation of insulin secretion, growth, and spermiogenesis. Proc Natl Acad Sci U S A. 2008; 105:2349–2353. [PubMed: 18268345]

Boden G. Obesity and free fatty acids. Endocrinol Metab Clin North Am. 2008; 37:635–646. viii–ix. [PubMed: 18775356]

Boucher J, K A, Kahn CR. Insulin receptor signaling in normal and insulin-resistant states. Cold Spring Harb Perspect Biol. 2014; 6:a009191. [PubMed: 24384568]

Brasaemle D. Thematic review series: adipocyte biology. The perilipin family of structural lipid droplet proteins: stabilization of lipid droplets and control of lipolysis. J Lipid Res. 2007; 48:2547–2559. [PubMed: 17878492]

Chakraborty A, K M, Bello NT, Maxwell M, Potter JJ, Juluri KR, Maag D, Kim S, Huang AS, Dailey MJ, Saleh M, Snowman AM, Moran TH, Mezey E, Snyder SH. Inositol pyrophosphates inhibit Akt signaling, regulate insulin sensitivity and weight gain. Cell. 2010; 143:897–910. [PubMed: 21145457]

Chakraborty A, K S, Snyder SH. Inositol pyrophosphates as mammalian cell signals. Sci Signal. 2011; 4:re1. [PubMed: 21878680]

Fu C, X J, Li RJ, Crawford JA, Khan AB, Ma TM, Cha JY, Snowman AM, Pletnikov MV, Snyder SH. Inositol Hexakisphosphate Kinase-3 Regulates the Morphology and Synapse Formation of Cerebellar Purkinje Cells via Spectrin/Adducin. J Neurosci. 2015; 35:11056–11067. [PubMed: 26245967]

Gauthier MS, M H, Souza SC, Cacicedo JM, Saha AK, Greenberg AS, Ruderman NB. AMP-activated protein kinase is activated as a consequence of lipolysis in the adipocyte: potential mechanism and physiological relevance. J Biol Chem. 2008; 283:16514–16524. [PubMed: 18390901]

Gokhale NA, Z A, Janoshazi AK, Weaver JD, Shears SB. PPIP5K1 modulates ligand competition between diphosphoinositol polyphosphates and PtdIns(3,4,5)P3 for polyphosphoinositide-binding domains. Biochem J. 2013; 453:413–426. [PubMed: 23682967]

Grujic D, S V, Harper ME, Himms-Hagen J, Cunningham BA, Corkey BE, Lowell BB. Beta3-adrenergic receptors on white and brown adipocytes mediate beta3-selective agonist-induced effects on energy expenditure, insulin secretion, and food intake. A study using transgenic and gene knockout mice. J Biol Chem. 1997; 272:17686–17693. [PubMed: 9211919]

Illies C, G J, Fiume R, Leibiger B, Yu J, Juhl K, Yang SN, Barma DK, Falck JR, Saiardi A, Barker CJ, Berggren PO. Requirement of inositol pyrophosphates for full exocytotic capacity in pancreatic beta cells. Science. 2007; 318:1299–1302. [PubMed: 18033884]

Koldobskiy MA, C A, Werner JK Jr, Snowman AM, Juluri KR, Vandiver MS, Kim S, Heletz S, Snyder SH. p53-mediated apoptosis requires inositol hexakisphosphate kinase-2. Proc Natl Acad Sci U S A. 2010; 107:20947–20951. [PubMed: 21078964]

Kozusko K, P S, Savage DB. Human congenital perilipin deficiency and insulin resistance. Endocr Dev. 2013; 24:150–155. [PubMed: 23392103]

Langin D. Adipose tissue lipolysis as a metabolic pathway to define pharmacological strategies against obesity and the metabolic syndrome. Pharmacol Res. 2006; 53:482–491. [PubMed: 16644234]

Lucas S, T G, Tiraby C, Mairal A, Langin D. Expression of human hormone-sensitive lipase in white adipose tissue of transgenic mice increases lipase activity but does not enhance in vitro lipolysis. J Lipid Res. 2003; 44:154–163. [PubMed: 12518034]

Mackenzie RW, E B. Akt/PKB activation and insulin signaling: a novel insulin signaling pathway in the treatment of type 2 diabetes. Diabetes Metab Syndr Obes. 2014; 13:55–64. [PubMed: 24611020]

Martinez-Botas J, A J, Tessier D, Lapillonne A, Chang BH, Quast MJ, Gorenstein D, Chen KH, Chan L. Absence of perilipin results in leanness and reverses obesity in Lepr(db/db) mice. Nat Genet. 2000; 26:474–479. [PubMed: 11101849]

McManaman JL, B E, Orlicky DJ, Jackman M, MacLean PS, Cain S, Crunk AE, Mansur A, Graham CE, Bowman TA, Greenberg AS. Perilipin-2-null mice are protected against diet-induced obesity, adipose inflammation, and fatty liver disease. J Lipid Res. 2013; 54:1346–1359. [PubMed: 23402988]

Morrison BH, H R, Lamarre E, Drazba J, Prestwich GD, Lindner DJ. Gene deletion of inositol hexakisphosphate kinase 2 predisposes to aerodigestive tract carcinoma. Oncogene. 2009; 28:2383–2392. [PubMed: 19430495]

Prasad A, J Y, Chakraborty A, Li Y, Jain SK, Zhong J, Roy SG, Loison F, Mondal S, Sakai J, Blanchard C, Snyder SH, Luo HR. Inositol hexakisphosphate kinase 1 regulates neutrophil function in innate immunity by inhibiting phosphatidylinositol-(3,4,5)-trisphosphate signaling. Nat Immunol. 2011; 12:752–760. [PubMed: 21685907]

Qiao L, K B, Schaack J, Shao J. Adiponectin inhibits lipolysis in mouse adipocytes. Diabetes. 2011; 60:1519–1527. [PubMed: 21430087]

Rao F, X J, Fu C, Cha JY, Gadalla MM, Xu R, Barrow JC, Snyder SH. Inositol pyrophosphates promote tumor growth and metastasis by antagonizing liver kinase B1. Proc Natl Acad Sci U S A. 2015

Roth Flach RJ, M A, Akie TE, Negrin KA, Paul MT, Czech MP. β3-Adrenergic receptor stimulation induces E-selectin-mediated adipose tissue inflammation. J Biol Chem. 2013; 288:2882–2892. [PubMed: 23235150]

Saha PK, K H, Martinez-Botas J, Sunehag AL, Chan L. Metabolic adaptations in the absence of perilipin: increased beta-oxidation and decreased hepatic glucose production associated with peripheral insulin resistance but normal glucose tolerance in perilipin-null mice. J Biol Chem. 2004; 279:35150–35158. [PubMed: 15197189]

Saiardi A, E-B H, Snowman AM, Tempst P, Snyder SH. Synthesis of diphosphoinositol pentakisphosphate by a newly identified family of higher inositol polyphosphate kinases. Curr Biol. 1999; 9:1323–1326. [PubMed: 10574768]

Shears S. Towards pharmacological intervention in inositol pyrophosphate signalling. Biochem Soc Trans. 2016; 44:191–196. [PubMed: 26862205]

Skinner JR, H L, Shew TM, Abumrad NA, Wolins NE. Perilipin 1 moves between the fat droplet and the endoplasmic reticulum. Adipocyte. 2013; 2:80–86. [PubMed: 23805403]

Szijgyarto Z, G A, Azevedo C, Saiardi A. Influence of inositol pyrophosphates on cellular energy dynamics. Science. 2011; 334:802–805. [PubMed: 22076377]

Tansey JT, S C, Gruia-Gray J, Roush DL, Zee JV, Gavrilova O, Reitman ML, Deng CX, Li C, Kimmel AR, Londos C. Perilipin ablation results in a lean mouse with aberrant adipocyte lipolysis, enhanced leptin production, and resistance to diet-induced obesity. Proc Natl Acad Sci U S A. 2001; 98:6494–6499. [PubMed: 11371650]

Taschler U, R F, Heier C, Schreiber R, Schweiger M, Schoiswohl G, Preiss-Landl K, Jaeger D, Reiter B, Koefeler HC, Wojciechowski J, Theussl C, Penninger JM, Lass A, Haemmerle G, Zechner R, Zimmermann R. Monoglyceride lipase deficiency in mice impairs lipolysis and attenuates diet-induced insulin resistance. J Biol Chem. 2011; 286:17467–17477. [PubMed: 21454566]

Thrush AB, G A, Sorisky A. PKC activation is required for TSH-mediated lipolysis via perilipin activation. Horm Metab Res. 2012; 44:825–831. [PubMed: 22730012]

Wilson MS, L T, Saiardi A. Inositol pyrophosphates: between signalling and metabolism. Biochem J. 2013; 452:369–379. [PubMed: 23725456]

Wong H, S M. The lipase gene family. J Lipid Res. 2002; 43:993–999. [PubMed: 12091482]

Wu M, D B, Trevisan AJ, Fiedler D. Synthesis and characterization of non-hydrolysable diphosphoinositol polyphosphate second messengers. Chem Sci. 2013; 4:405–410. [PubMed: 23378892]

Xu Y, L H, Bajrami B, Kwak H, Cao S, Liu P, Zhou J, Zhou Y, Zhu H, Ye K, Luo HR. Cigarette smoke (CS) and nicotine delay neutrophil spontaneous death via suppressing production of

diphosphoinositol pentakisphosphate. Proc Natl Acad Sci U S A. 2013; 110:7726–7731. [PubMed: 23610437]

Young SG, Z R. Biochemistry and pathophysiology of intravascular and intracellular lipolysis. Genes Dev. 2013; 27:459–484. [PubMed: 23475957]

Zebisch K, V V, Wabitsch M, Brandsch M. Protocol for effective differentiation of 3T3-L1 cells to adipocytes. Anal Biochem. 2012; 425:88–90. [PubMed: 22425542]

Zhang Z, L D, Gao X, Zhao C, Qin X, Xu Y, Su T, Sun D, Li W, Wang H, Liu B, Cao F. Selective inhibition of inositol hexakisphosphate kinases (IP6Ks) enhances mesenchymal stem cell engraftment and improves therapeutic efficacy for myocardial infarction. Basic Res Cardiol. 2014a; 109:417. [PubMed: 24847908]

Zhang Z, Z C, Liu B, Liang D, Qin X, Li X, Zhang R, Li C, Wang H, Sun D, Cao F. Inositol pyrophosphates mediate the effects of aging on bone marrow mesenchymal stem cells by inhibiting Akt signaling. Stem Cell Res Ther. 2014b; 5:33. [PubMed: 24670364]

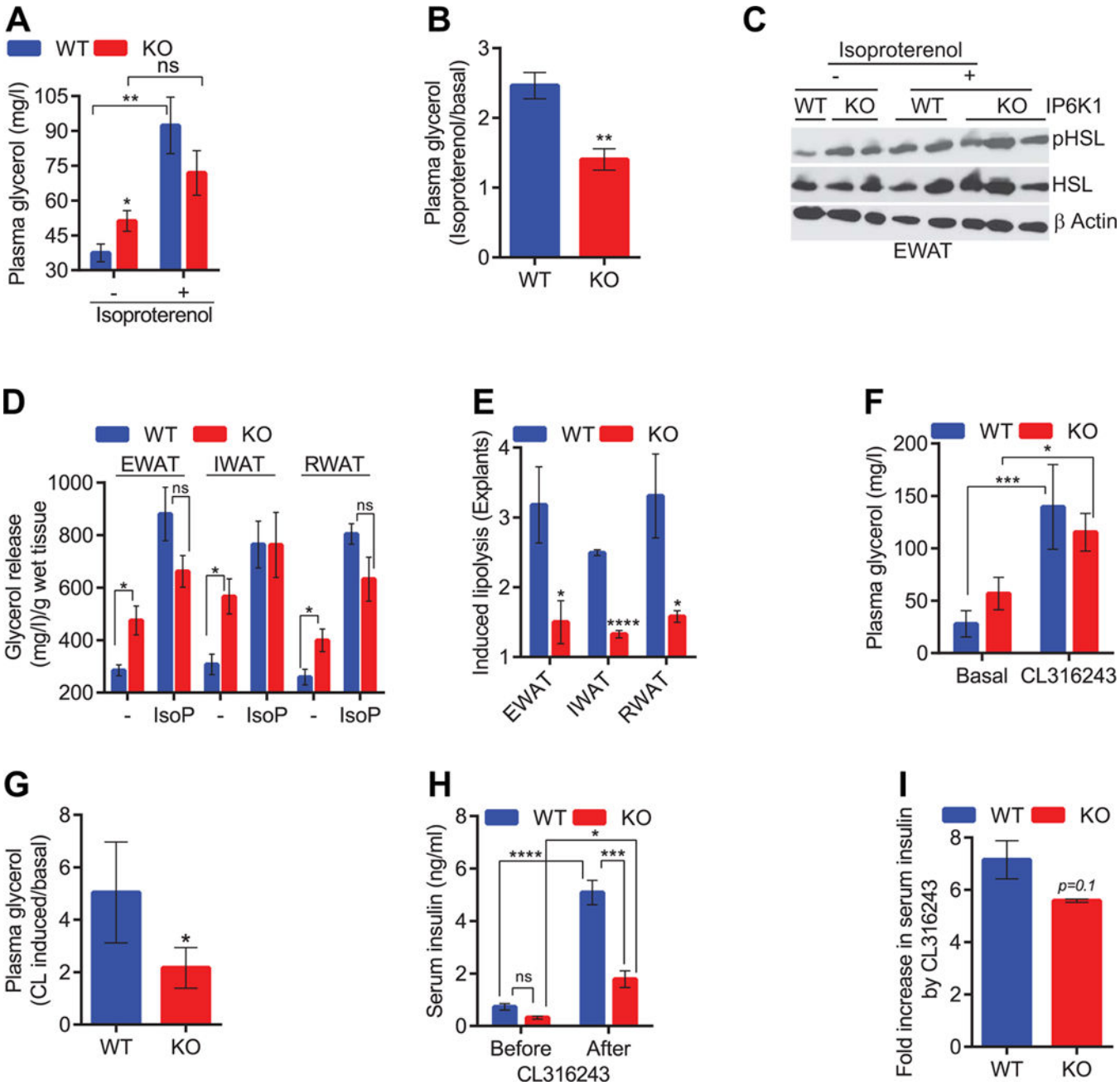

Figure 1. IP6K1-KO mice display altered lipolysis

A. Plasma glycerol is significantly higher in overnight fasted IP6K1-KO mice which is enhanced to a slightly lesser extent by isoproterenol treatment (n=5/group).

B. The ratio of isoproterenol induced *vs* basal plasma glycerol is reduced in IP6K1-KO mice.

C. The stimulatory phosphorylation of HSL (S660) is higher in the IP6K1-KO EWAT under basal condition. Isoproterenol induces HSL phosphorylation in the WT albeit not in the knockouts.

D. Explants of EWAT, IWAT and RWAT of IP6K1-KO mice release more glycerol than WT under basal condition whereas isoproterenol (IsoP) induced release is not significantly altered (n=3/group).

E. The ratio of isoproterenol induced vs basal glycerol release is less in adipose tissue explants isolated from IP6K1-KO mice.

F. Plasma glycerol level is marginally higher in ad libitum IP6K1-KO mice compared to WT. CL316243, similar to isoproterenol induces lipolysis to a slightly lesser extent in the knockouts (n=4).

G. The ratio of CL316243 induced vs basal lipolysis is significantly less in IP6K1-KO mice.

H. Plasma insulin level is slightly lower in ad libitum IP6K1-KO mice. CL316243 enhances insulin level in both WT and IP6K1-KO mice (n=3/group).

I. CL316243 mediated enhancement in plasma insulin level is marginally less in the knockouts.

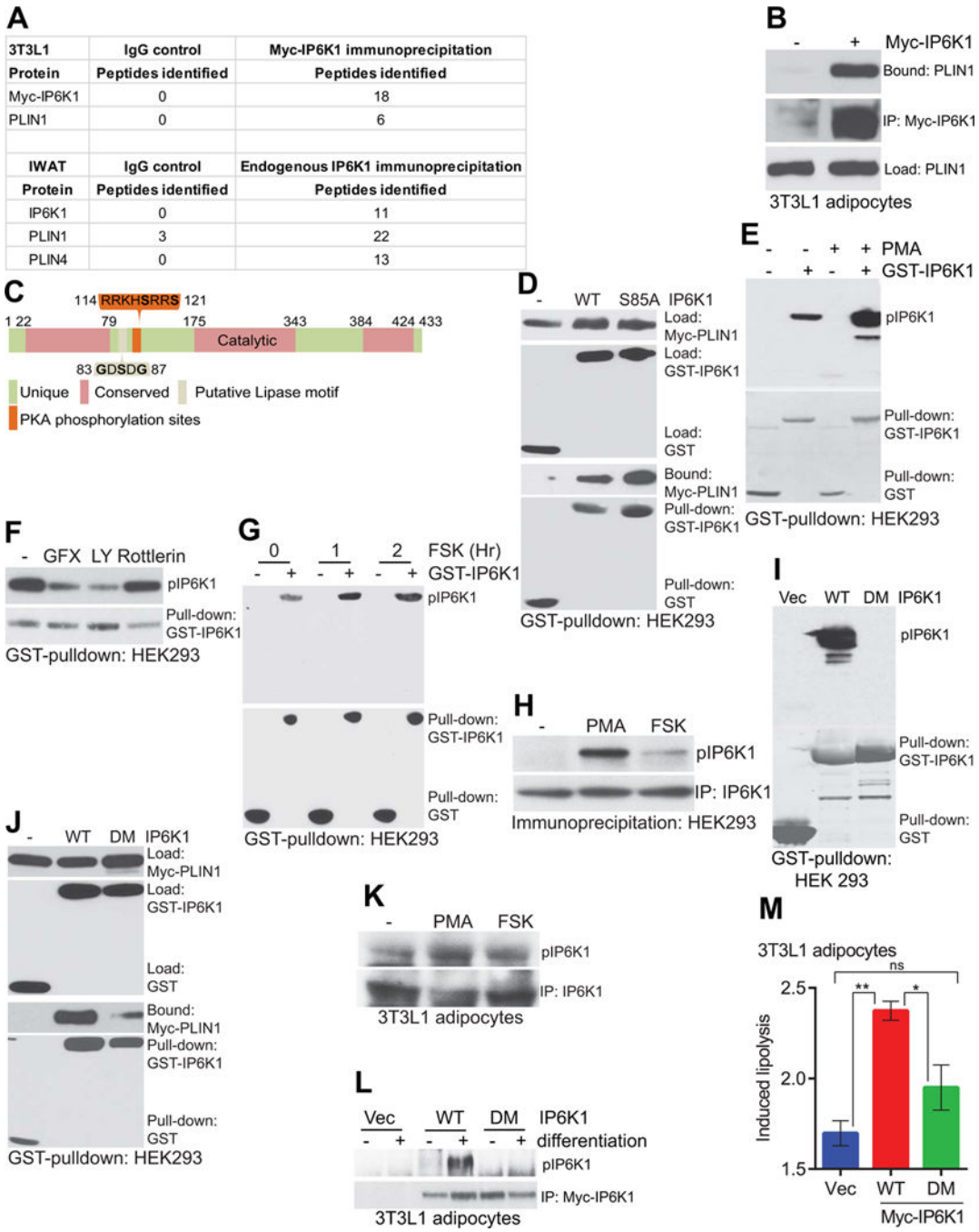

Figure 2. A PKA/PKC phosphorylation motif in IP6K1 regulates its interaction with PLIN1 and lipolysis

A. Mass spectrometry identified PLIN1 as an interactor of overexpressed Myc-IP6K1 in the 3T3L1 adipocytes (top panel). PLIN1 and PLIN4 also interact with endogenous IP6K1 in the IWAT (bottom panel).

B. Co-immunoprecipitation followed by immunoblotting confirm that PLIN1 interacts with Myc-IP6K1 in 3T3L1 adipocytes.

C. Schematic representation of IP6K1 protein sequence. Amino acid sequences which are conserved among three IP6K isoforms are denoted in pink. Unique sequences are

represented as green. IP6K1 possesses a lipase like motif (GDSDG) and a PKC/PKA phosphorylation motif (KHSRRS) in the unique region.

D GST-IP6K1-S85A (putative lipase motif mutant) does not influence its binding to Myc-PLIN1 in HEK293 cells.

E. GST-IP6K1 is basally phosphorylated in HEK293 cells which is further enhanced by pharmacologic stimulation of PKC by the phorbol ester PMA.

F. The pan PKC inhibitor GFX109203X or the PKCβ specific inhibitor LY333531 reduce GST-IP6K1 phosphorylation in HEK293 cells whereas the PKCδ inhibitor rottlerin does not exert any effect.

G. GST-IP6K1 phosphorylation in HEK293 cells is enhanced by forskolin (FSK) mediated PKA activation.

H. Endogenous IP6K1 phosphorylation in HEK293 cells is enhanced to a greater extent by PKC activation compared to PKA activation as evidenced by PMA and FSK treatments.

I. Phospho-PKC substrate specific antibody fails to detect phosphorylation of IP6K1-DM (S118A–S121A) in HEK293 cells.

J. IP6K1-DM does not efficiently bind Myc-PLIN1 in HEK293 cells.

K. Endogenous IP6K1 phosphorylation is enhanced by pharmacologic PKC or PKA activation in 3T3L1 adipocytes.

L. IP6K1-WT is phosphorylated in mature 3T3L1 adipocytes. IP6K1-DM is not phosphorylated. − and + denote undifferentiated and differentiated states.

M. The ratio of isoproterenol induced vs basal glycerol release is higher in IP6K1-WT overexpressed 3T3L1 adipocytes compared to IP6K1-DM expressing cells.